

313-91
14073/
p-24

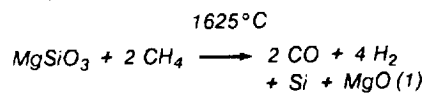
The Onsite Manufacture of Propellant Oxygen From Lunar Resources

Sanders D. Rosenberg; Robert L. Beegle, Jr.;
Gerald A. Guter; Frederick E. Miller; and Michael Rothenberg

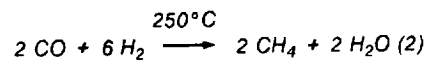
Figure 7

Oxygen From Lunar Silicates

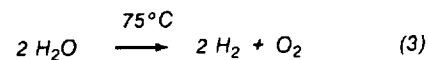
The first of the three steps in the process of carbothermal reduction of silicates takes place in the silicate reduction reactor. Magnesium silicate, which typifies lunar rock, is reduced to carbon monoxide, silicon, and slag, using methane as the reducing agent. The step requires a very high temperature: 1625°C.



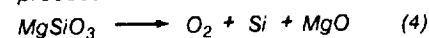
In the second step, the carbon monoxide is catalytically reduced with hydrogen to regenerate the methane and form water. This step takes place at the relatively low temperature of 250°C.



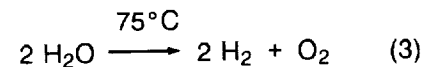
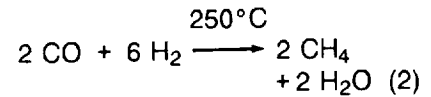
In the final step, the water is condensed to a liquid (at 75°C) and electrolyzed to regenerate the hydrogen used in step 2 and to produce the desired oxygen.



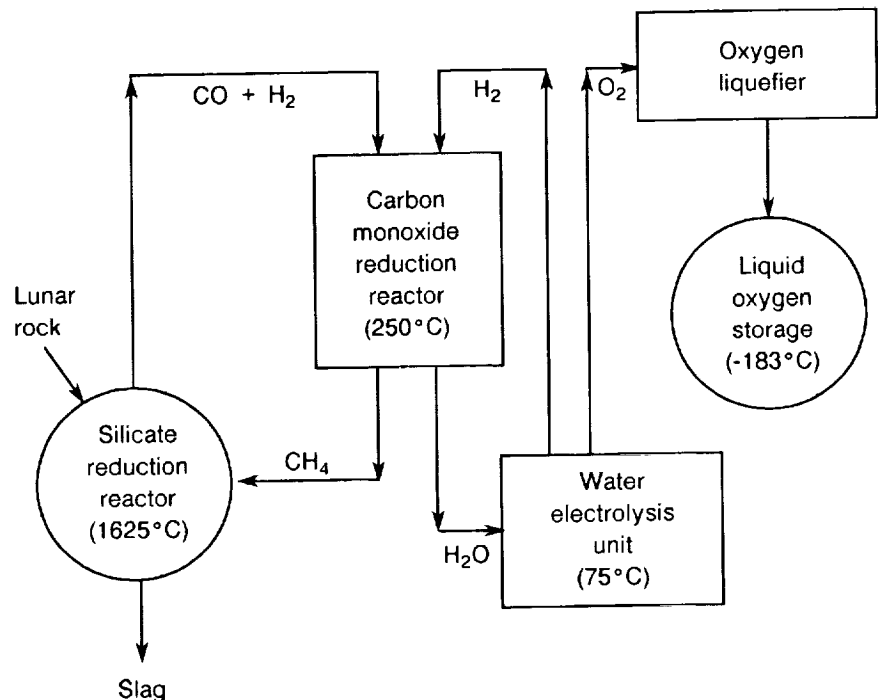
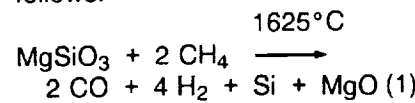
Since the methane and hydrogen are regenerated and recycled, this process ideally uses up only energy and the input metal silicates. Thus, the following reaction can be seen as the sum of the process.



The Aerojet carbothermal process for the manufacture of oxygen from lunar materials has three essential steps: the reduction of silicate with methane to form carbon monoxide and hydrogen, the reduction of carbon monoxide with hydrogen to form methane and water, and the electrolysis of water to form hydrogen and oxygen. The reactions are as follows:



The overall process is shown in figure 7. Figure 8 is a schematic flow diagram of the silicate reduction furnace used in this program.



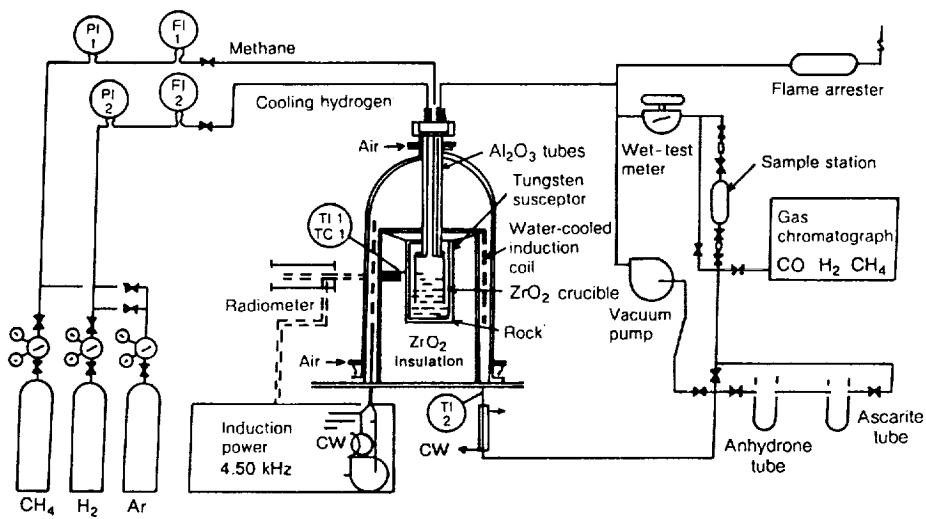


Figure 8

Silicate Reduction Furnace

- TI = temperature indicator
- TC = temperature controller
- PI = pressure indicator
- FI = flow indicator
- CW = cold water

Reduction of Igneous Rock With Carbon and Silicon Carbide

A series of reactions of basalt and granite with carbon and silicon carbide were carried out to determine the temperature profile for the reduction reactions that may occur during the reduction of igneous rock with methane. The results of three of these runs are illustrated in figure 9.

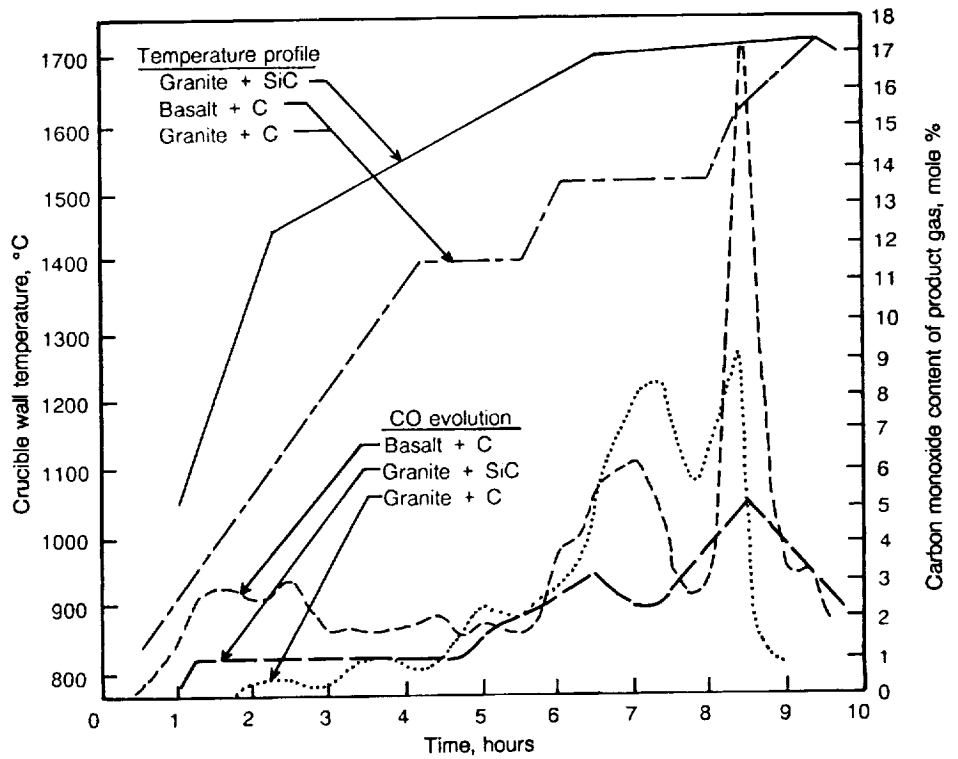


Figure 9

Reduction of Basalt and Granite With Carbon and Silicon Carbide

In the reaction of basalt (50 g) with carbon (5 g), the initial evolution of carbon monoxide resulted from the reduction of iron oxide. The basalt contained 11.86 percent iron oxide (as Fe_2O_3); the reduction of this oxide, if present as Fe_2O_3 , would require 1.34 g of carbon. The carbon monoxide that evolved during the first 2.5 hours represented 1.0 g of the carbon. Other reducible materials present in the basalt were titanium dioxide (2.47%) and sodium oxide (3.73%). These oxides would consume 0.43 g of carbon. Consequently, only 35 percent of the carbon could have been oxidized by materials other than silicon dioxide. The recovery in the form of carbon monoxide of 89.1 percent of the carbon with which the reactor was charged indicates that a considerable portion of the silicon dioxide present in the basalt was reduced at temperatures as low as 1550°C.

Three solid products were obtained: slag and metal remained in the zirconium dioxide crucible and sublimate was found at the top of the bell jar. The slag was composed mainly of aluminum oxide. The composition of the metal was 82 percent iron, 13 percent silicon, and minor amounts of titanium, vanadium, nickel, and copper. Of the sublimate, 61 percent was sodium, which is highly volatile.

In the reaction of granite (50 g) with carbon (5 g), much less

carbon monoxide was produced at low temperature. This result is due to the lower percentages of reducible oxides in the granite; that is, iron oxide (2.05% as Fe_2O_3), sodium oxide (3.10%), and potassium oxide (4.90%). Complete reduction of these oxides would consume 0.85 g (17%) of the carbon introduced. A total of 73 percent of the carbon introduced was recovered as carbon monoxide; therefore, we conclude that silicon dioxide reduction accounts for most of the carbon monoxide evolved at 1550°C and higher temperatures.

We believe that most of the rest of the carbon introduced reacted with silicon to form silicon carbide. The slag had nonmagnetic pieces of metal dispersed throughout and contained 2.3 percent carbon; that is, 20 percent of the carbon introduced.

In the reaction of granite (37.5 g) with silicon carbide (12.5 g), almost no reaction occurred below 1100°C; about 7 percent of the silicon carbide was reacted between 1100 and 1500°C. As the temperature was increased from 1500 to 1740°C, the reaction rate gradually increased and then rapidly decreased when most of the carbon was consumed. About 83 percent of the carbon in the silicon carbide was recovered as carbon oxides. The dark, metallic looking slag contained an additional 10 percent of the carbon introduced as silicon carbide.

Figure 10

CO-H₂ Reduction Unit

- DP = differential pressure transducer
- FCR = flow control recorder
- GC = gas chromatograph
- PC = pressure controller
- PI = pressure indicator (gauge)
- PS = pressure switch
- RV = relief valve
- ⊙ = gas sample
- ⊠ = solenoid valves
- ΔT = Δ temperature recorder
- TC = thermocouple
- TI = temperature indicator (thermocouple point)
- WTM = wet-test meter

Analysis of the metal recovered from the melt gave 59 percent iron, 28 percent silicon, and minor amounts of titanium, vanadium, nickel, and copper. The slag was composed mainly of aluminum oxide and silicon dioxide.

These results indicate that, if silicon carbide is formed by reaction of granite and carbon, excess granite will react with the carbide to produce silicon and carbon monoxide. The rate of the granite-silicon carbide reaction at 1740°C is comparable to that of the granite-carbon reaction at 1625°C.

Reduction of Carbon Monoxide With Hydrogen

The reduction of carbon monoxide with hydrogen to form methane and water was studied using a nickel-on-kieselguhr catalyst. A schematic flow diagram of the hydrogen-carbon monoxide reactor used in this program is shown in figure 10. The data for these runs are presented in tables 1 to 5 and figures 11 to 13. The various parameters that were studied are discussed in the following paragraphs.

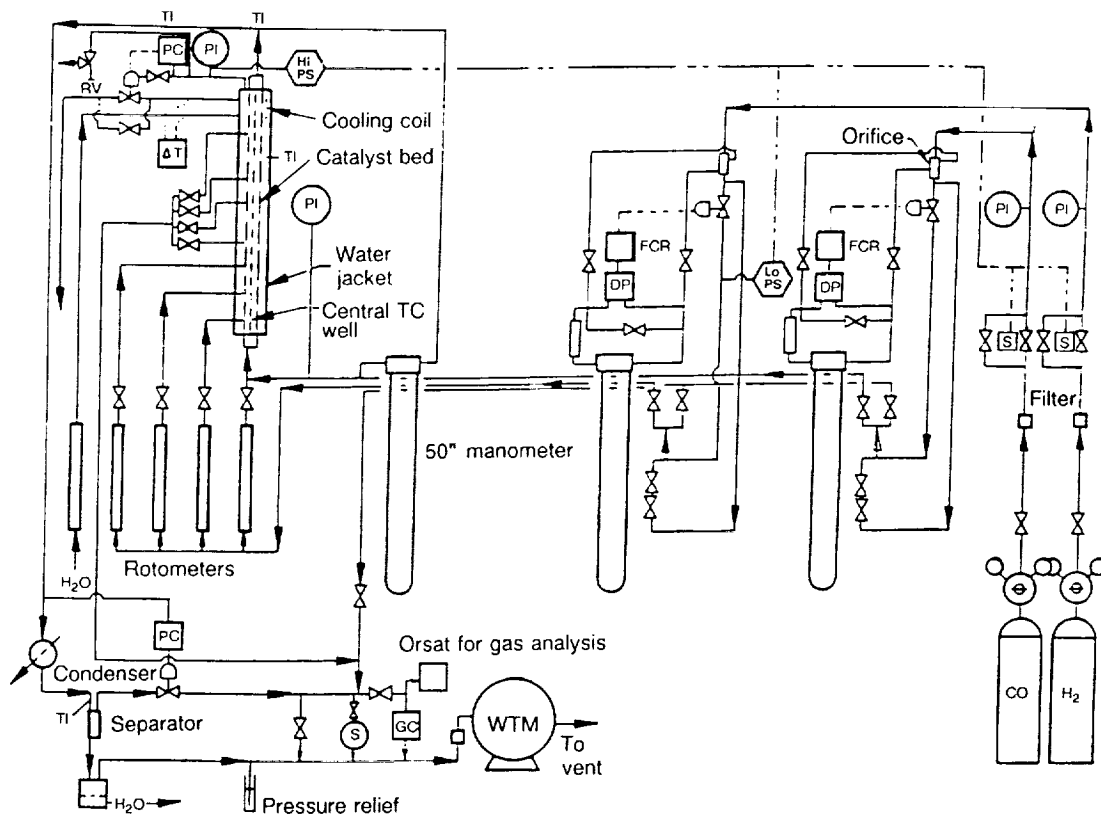


TABLE 1. Reduction of Carbon Monoxide With Hydrogen To Form Water and Methane (and CO₂):
Results of Selected Runs Between 45 and 57

Run	H ₂ /CO mole ratio	Space velocity, hr ⁻¹	Catalyst bed pressure, atm	Catalyst bed temp., °C	Material balance, %	CO conversion, mole %	Normalized product yield, mole %		
							H ₂ O	CH ₄	CO ₂
45	4.00	500	1.0	250	101.0	100.0	100.0	100.0	0.0
46	4.00	750	1.0	249	93.3	100.0	100.0	100.0	0.0
47	4.10	1003	1.0	252	99.0	100.0	100.0	100.0	0.0
48	3.96	1481	1.0	253	95.3	100.0	99.8	99.9	0.1
49a	4.06	1000	1.0	251	101.0	100.0	100.0	100.0	0.0
51	4.15	2010	1.0	265	98.6	100.0	100.0	100.0	0.0
52b	2.84	810	1.0	248	98.1	100.0	91.1	96.2	3.7
53	3.56	1000	1.0	254	94.5	100.0	100.0	100.0	0.0
54	3.14	998	1.0	254	95.0	100.0	98.3	99.1	0.8
55	3.03	1000	6.1	253	96.9	100.0	99.2	99.4	0.4
56	3.01	1500	6.1	231	95.4	100.0	97.3	98.5	1.3
57	3.02	1500	6.1	353	94.8	100.0	94.8	97.1	2.5

TABLE 2. Analysis of the Gases Produced in the Reduction of
Carbon Monoxide With Hydrogen, Selected Runs 45-57

Run	Composition of product gas, vol. %				
	H ₂	H ₂ O	CO	CH ₄	CO ₂
45	49.4	1.20	0.0	49.4	0.00
46	49.4	1.15	0.0	49.4	0.00
47	51.5	1.15	0.0	47.3	0.00
48	48.4	1.15	0.0	50.4	0.05
49a	50.8	1.15	0.0	48.1	0.00
51	53.0	1.15	0.0	45.9	0.00
52b	8.9	1.14	0.0	91.5	3.50
53	38.5	1.14	0.0	60.4	0.00
54	17.7	1.14	0.0	80.5	0.65
55	9.3	0.20	0.0	90.2	0.35
56	12.0	0.20	0.0	96.6	1.27
57	18.9	0.20	0.0	78.6	2.25

TABLE 3. *Reactant Gas Carbon Dioxide Content vs. Catalyst Bed Length*

Run	Space velocity, hr ⁻¹	H ₂ /CO mole ratio	CO ₂ analysis, vol. %		
			Initial third	Middle third	Outlet
45	500	4.0	0.4	0.0	0.00
46	750	4.0	1.6	0.0	0.00
47	1000	4.1	2.7	0.3	0.00
48	1481	4.0	4.6	0.8	0.05
51	2010	4.1	3.8	0.2	0.00
55	1000	3.0	4.9	1.0	0.35
57	1500	3.0	6.1	3.6	2.25

TABLE 4. *Reduction of Carbon Monoxide With Hydrogen To Form Water and Methane (and CO₂): Results of Selected Runs Between 63 and 67*

Run	Impurity mole % in H ₂ stream	H ₂ /CO mole ratio	Space velocity hr ⁻¹	Catalyst bed pressure, atm	Catalyst bed temp., °C	Material balance, %	CO conversion, mole %	Normalized product yield, mole %		
								H ₂ O	CH ₄	CO ₂
63b	None	3.00	1000	6.1	254	99.5	100.0	97.6	99.0	0.95
64c	0.1 COS	3.00	1000	6.1	254	97.1	100.0	96.4	98.2	1.65
66b	1.0 NO	2.98	1005	6.1	255	98.8	100.0	98.6	97.2	1.87
66c	1.0 NO	3.44	1120	6.1	252	100.8	100.0	100.0	100.0	0.00
67b	0.5 PH ₃	3.09	1024	6.1	249	100.6	100.0	97.2	98.2	1.52

TABLE 5. Analysis of the Gases Produced in the Reduction of Carbon Monoxide With Hydrogen, Selected Runs 63-67

Run	Composition of product gas, vol. %						
	H ₂	H ₂ O	CO	CH ₄	CO ₂	NH ₃	N ₂
63b	6.0	0.20	0.0	92.9	0.9	----	----
64c	5.0	0.20	0.0	93.2	1.6	----	----
66b	4.0	0.20	0.0	93.3	1.8	0.2	0.5
66c	21.8	0.20	0.0	77.2	0.0	0.3	0.5
67b	10.0	0.20	0.0	88.4	1.4	----	----

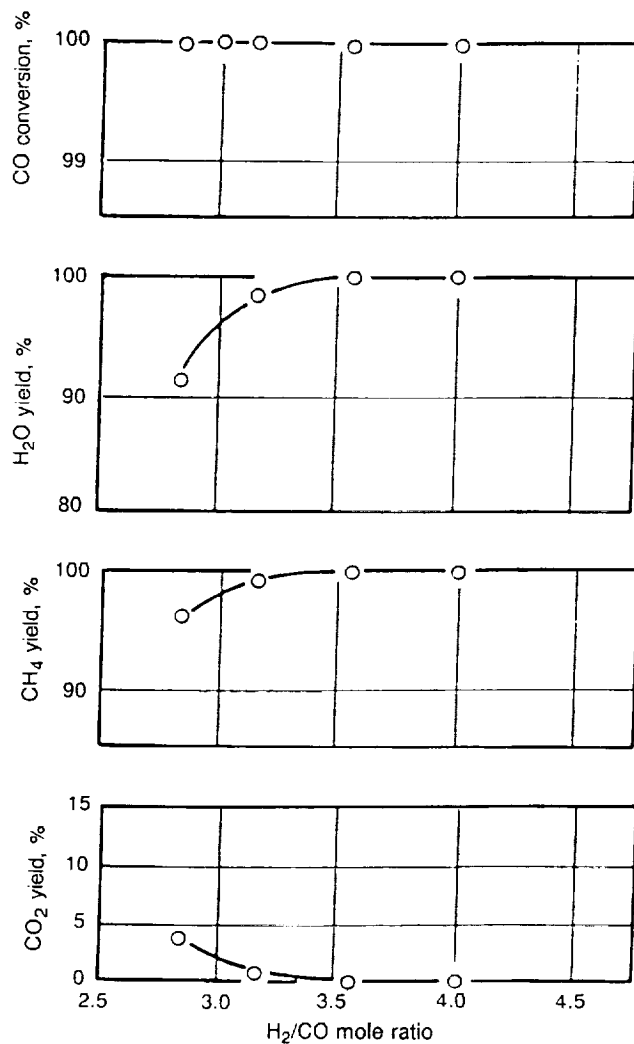


Figure 11

Carbon Monoxide Conversion and Yields vs. Hydrogen-Carbon Monoxide Mole Ratio (1000 hr⁻¹ space velocity; 250° C; 1.0 atm)

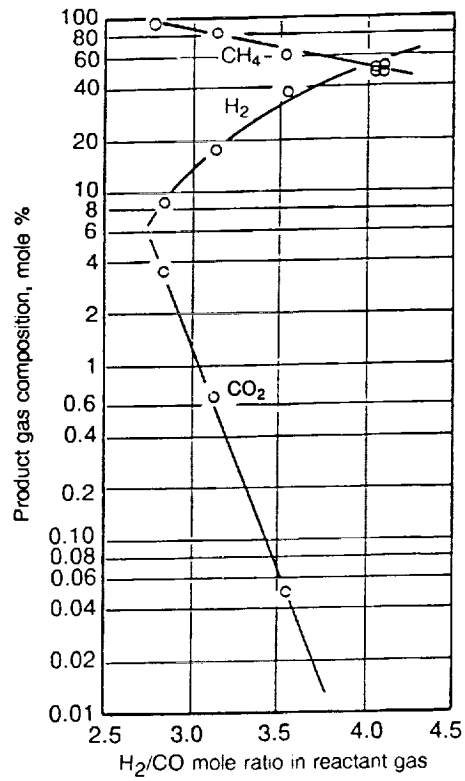


Figure 12

Product Gas Composition vs. Hydrogen-Carbon Monoxide Mole Ratio (1000 hr⁻¹ space velocity; 250°C; 1.0 atm)

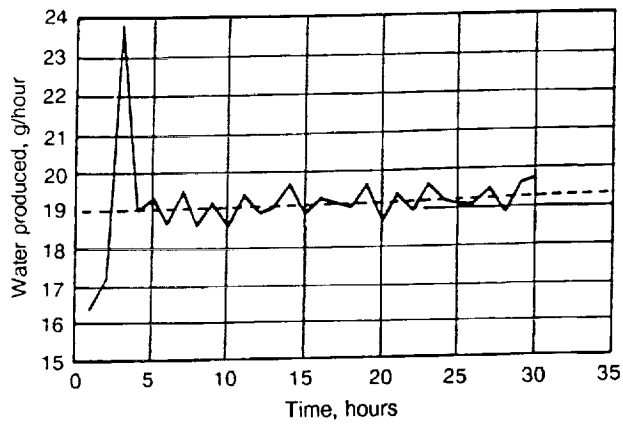


Figure 13

Water Production Rate vs. Time for Run 49 (1000 hr⁻¹ space velocity; 250°C; 1 atm; 4:1 mole ratio)

Temperature

Some catalyst activity was noted as low as 200°C; the catalyst was found to be very active at 250°C; so excellent conversions were obtained. Therefore, all the runs were made at a nominal catalyst bed temperature of 250°C, except run 57, which was made at 350°C. In run 57 we tried to increase the conversion at a 3:1 hydrogen-carbon monoxide mole ratio and a 1500-hr⁻¹ space velocity by increasing the temperature; however, the conversion of carbon dioxide to methane and water decreased as the temperature was increased.

Pressure

The first nine runs were made at atmospheric pressure. The conversions were nearly complete at a 4:1 mole ratio even with space velocities of 2000 hr⁻¹. It was only at lower hydrogen-carbon monoxide mole ratios that the conversions decreased sufficiently to require raising the catalyst bed pressure. The last three runs were made at 6.1 atm to approach complete conversion at a 3:1 ratio. In comparing runs 54 and 55, it can be seen that increasing the pressure from 1 to 6 atm decreased the carbon dioxide yield from 0.8 to 0.4 percent and correspondingly increased the yields of water and methane.

Hydrogen-Carbon Monoxide Mole Ratio

The effect of hydrogen-carbon monoxide mole ratio on conversion and yields can be seen in figure 11. At a space velocity of 1000 hr⁻¹, at 250°C and 1.0 atm, the catalyst gave complete conversion of carbon monoxide and carbon dioxide until we decreased the hydrogen-carbon monoxide mole ratio to less than 3.5:1. The carbon monoxide conversion remained complete but the carbon dioxide yield increased; at a 3:1 ratio, the carbon dioxide yield was approximately 2 percent.

The effect of hydrogen-carbon monoxide mole ratio on the product gas composition can be seen in figure 12. No carbon monoxide could be detected in the outlet gas for any of these runs. Within this range, the carbon dioxide content of the gas increased logarithmically as the hydrogen-carbon monoxide mole ratio was decreased below 3.5:1 (to about 1.5% at 3:1). The theoretical product yield at a 3:1 ratio is 100 percent methane, 0 percent hydrogen. The catalyst gave 86 percent methane, 13 percent hydrogen at the 3:1 ratio.

Space Velocity*

At a 4:1 mole ratio, no carbon dioxide was formed at space velocities up to 2000 hr⁻¹. At a 3:1 ratio, the carbon dioxide yield increased rapidly as the space velocity was increased above 1000 hr⁻¹.

Material Balance

With the exception of two runs, all overall material balances for the runs (see table 1) were under 100 percent. Most of the low material balances can be attributed to low water recoveries. Because the catalyst is known to be a good adsorbent for water, we hypothesized that some of the water was slowly being adsorbed on the catalyst. In order to prove that this was the case, a long-duration run (run 49) was made. See figure 13. The water production, which fluctuated about ± 0.5 g/hr, gradually increased throughout the run (dotted line). After 30 hours, the liquid water production rate was 19.2 g/hr (about 96% of theoretical). At the rate of increase of water production (0.01 g/hr), it would have taken about 100 hr before the actual water production rate equaled the theoretical production rate. For long runs, the water

balance should be no problem; in fact, we hypothesize that the small amount of water adsorbed on the catalyst may help to prevent carbon formation.

Heat Balance

In all runs, the majority of the heat was released in the initial third of the bed; however, in several runs at high space velocity (1500 or 2000 hr⁻¹) or low hydrogen-carbon monoxide mole ratios (3:1) or both, enough heat was released in the middle third of the catalyst bed to require some cooling. At the highest space velocities, temperature control was very difficult, because of the large amount of cooling air required to maintain the nominal catalyst bed temperature.

Pressure Drop

The relatively low pressure drop across the catalyst bed was excellent. It did not go up with time even at hydrogen-carbon monoxide mole ratios as low as 3:1. Run 49 was continued for 31 hours without shutdown; the pressure drop did not increase a measurable amount during this long period. The absence of a pressure buildup at the catalyst bed indicated no carbon deposition and a long, useful catalyst life.

* *Space velocity* is a measure of reactor capacity. It is the reciprocal of *space time*, which is defined as the time elapsed in processing one reactor volume of feed at specified conditions. Thus, *space velocity* is the number of reactor volumes of feed that can be processed within a given time. The higher the space velocity the better, provided the desired reaction occurs.

Catalyst Life

The catalyst was still active when it was removed after 14 runs (110 hr). As can be seen from the tabulation below, analyses of the catalyst before and after use showed no carbon deposition.

Time, hr	Carbon content of catalyst C-0765-1001-1, wt. %
0	5.08
110, initial third	5.02
110, middle third	5.11

As stated previously, there was no pressure buildup during the run, so this would not be a limiting factor on the life of the catalyst.

However, impurities in the feed may prove to be a limiting factor. Temperature control is also vital, because carbon is definitely deposited on the catalyst at higher temperatures (400°C and up). Catalyst life would probably be extended if the operating temperatures were started low when the catalyst was new and active and then gradually raised as the catalyst activity declined.

Catalyst Bed Length

At low space velocities, only the first inch or two of the catalyst bed was involved in the major portion

of the reaction. As the space velocity was increased, more and more of the bed was involved until, at very high space velocities and low hydrogen-carbon monoxide mole ratios (runs 55 and 57), even the full length of the catalyst bed was unable to achieve complete conversion of carbon dioxide into methane and water. This effect is best shown by carbon dioxide gradients in the reactor taken for the various runs, as reported in table 3. Two additional advantages of a long catalyst bed are that it allows a margin of safety as the catalyst ages and becomes less active and that it allows the initial portion of the bed to act as a guard chamber to remove various catalyst poisons.

Lunar Surface Plant Design

Estimates of the weight and power requirements for a lunar surface plant using the Aerojet carbothermal process are given in this section of the paper. In making these estimates, we assumed that no water is present in, or obtainable from, the lunar material. Large differences in weight result when different cooling methods are employed, because of the large amount of waste heat produced.

Heat Rejection

Two different methods of heat rejection were considered in this study:

1. A dual-cycle refrigeration system to "pump" the heat up to a high rejection temperature
2. Direct heat rejection by radiation to space

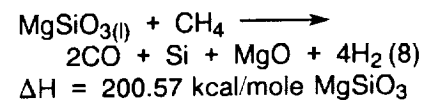
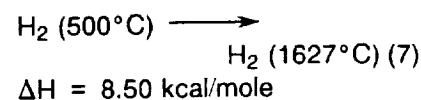
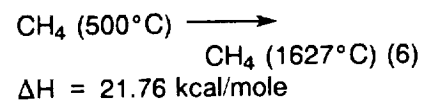
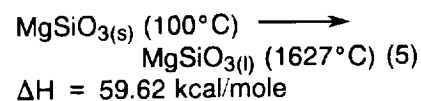
The first method is based on standard refrigeration principles. It employs *n*-butane as the primary refrigerant, with water as the secondary refrigerant and the medium for transferring heat to a space radiator. Refrigeration is not used in the second method. Instead, we assume that a radiator is able to reject heat directly into 0 K space.

In the estimates for the different sections of the process, power requirements are given for these two different methods of cooling. In the following tables and figures, method 1 indicates the refrigerative

technique and method 2 indicates the radiative technique. The details of the two methods are discussed later in this paper.

Reduction of Silicates With Methane

The estimates of heat and power requirements are based on the following changes:



The process flowsheet for this section is shown in figure 14.

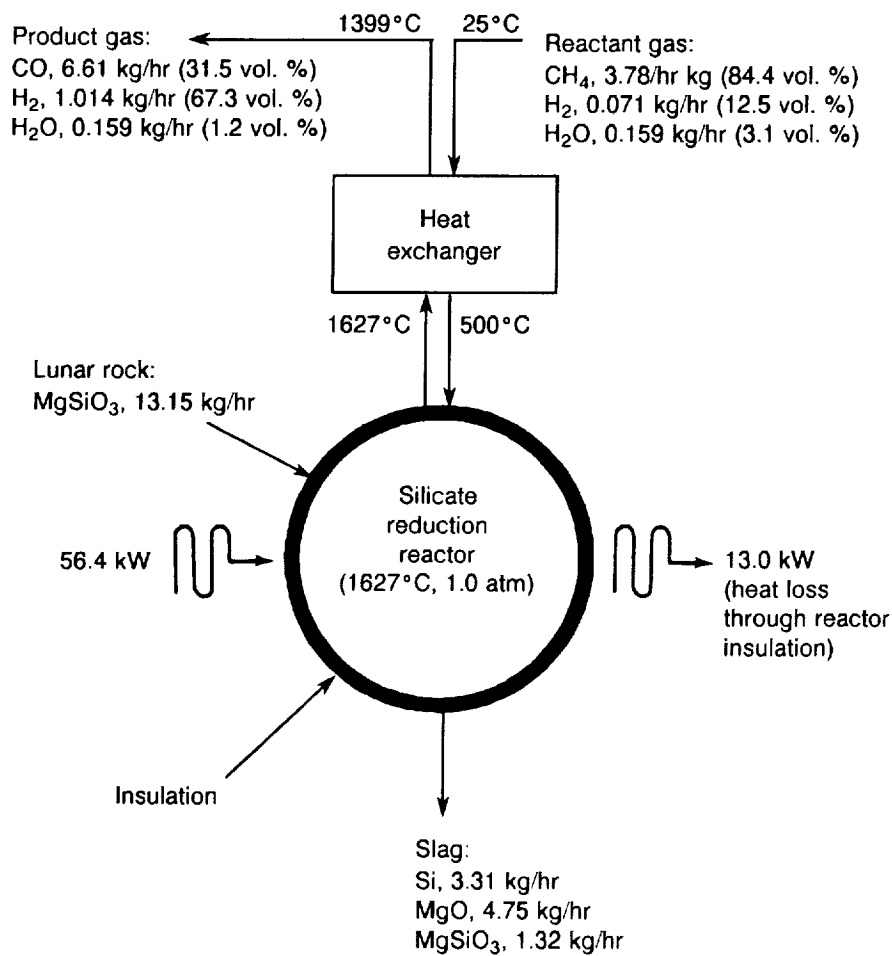
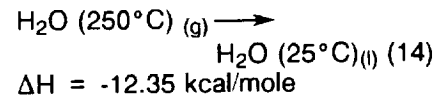
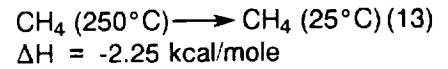
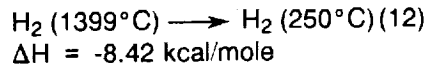
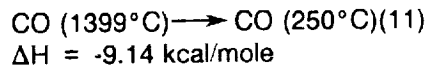
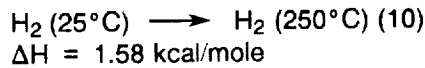
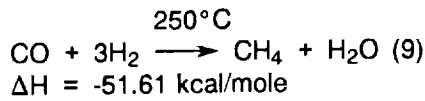


Figure 14

Silicate Reduction Reactor Section

Reduction of Carbon Monoxide

The estimates of heat and power requirements are based on the following changes:



The process flowsheet for this section is shown in figure 15. The operating temperature of 250°C is used as a conservative value. Operating at higher temperature offers a modest advantage in reducing radiator weight.

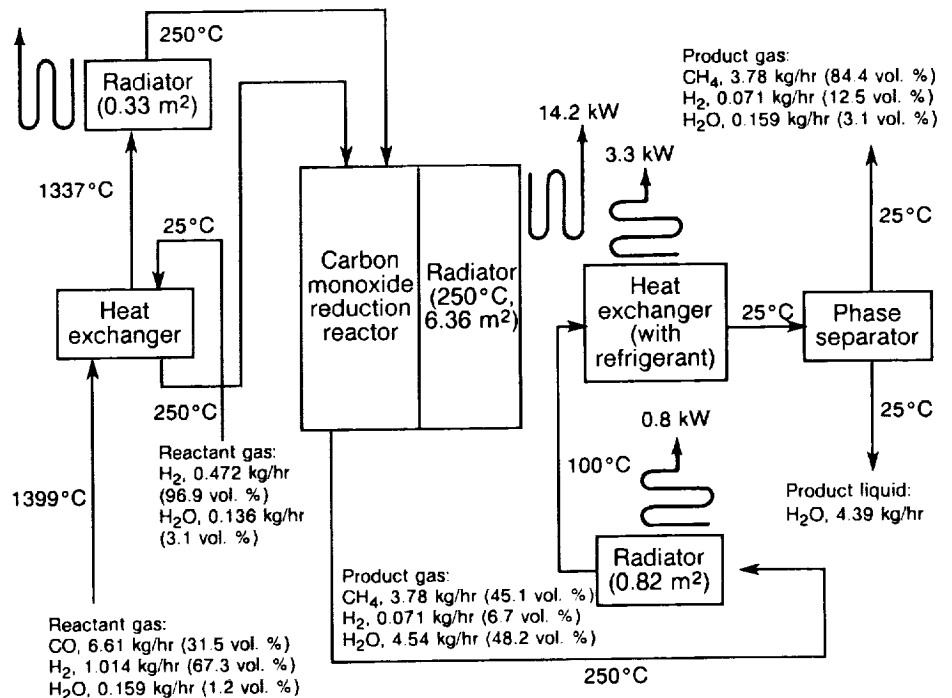


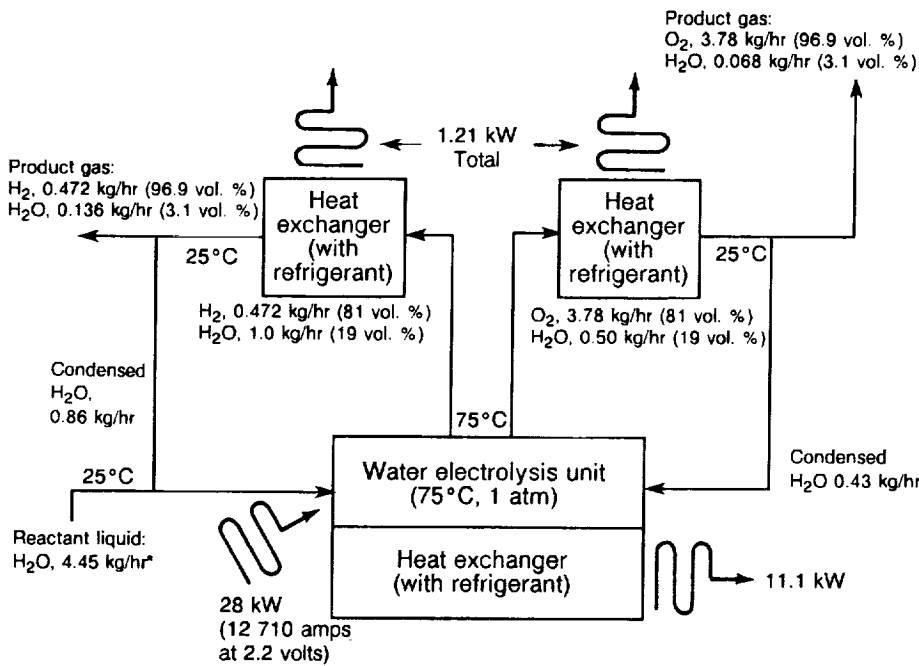
Figure 15

Carbon Monoxide Reduction Section

Water Electrolysis

Most of the weight of the electrolysis unit is that of the refrigeration cooling system and radiators used to reject low-temperature heat. The details of this section are shown in figure 16. A high-pressure electrolysis unit will allow operation at higher temperatures and higher efficiencies—a situation

advantageous for both weight and power savings. However, the high-pressure electrolysis unit itself is heavier than a low-pressure unit and, because of added corrosion problems, requires considerably more maintenance. Consequently, detailed tradeoff analysis of low-pressure versus high-pressure electrolysis is needed.



* 4.25 kg/hr required for electrolysis
 0.136 kg/hr recycled with hydrogen steam
 0.068 kg/hr condensed in liquid oxygen cold trap and returned to electrolysis unit intermittently

Figure 16

Water Electrolysis Section

Oxygen Liquefaction

The oxygen liquefaction system is composed of Norelco type 12080 gas liquefiers. These units use helium as a refrigerant; some makeup helium is required. The details of this section are shown in figure 17. The amount of helium indicated in the tables is for a 1-year operation.

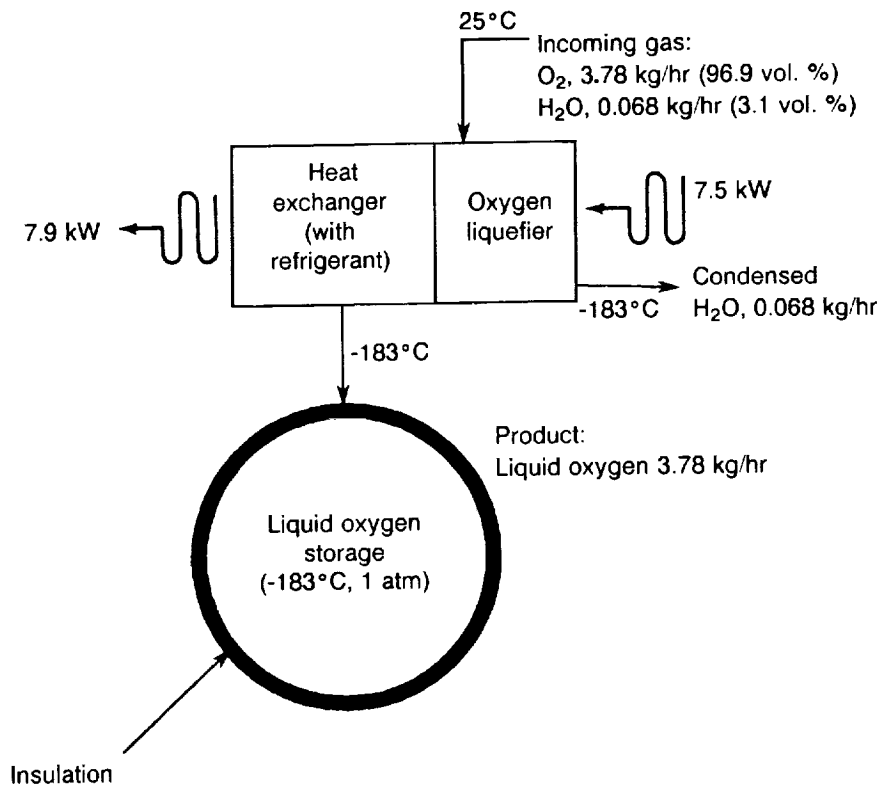


Figure 17

Oxygen Liquefaction and Storage Section

Oxygen Storage

The oxygen storage system consists of spheres of aluminum with walls 1.02 cm thick and an outer diameter of 3.20 m. Each sphere is capable of containing a 6-month supply of oxygen when it is produced at a rate of 2721 kg/month. These spheres are insulated to reduce boiloff. Boiloff oxygen is recondensed and returned to storage. The utilization of empty oxidizer storage tanks on lunar landing vehicles may eliminate the need for these

storage spheres. Figure 17 summarizes the details of this section.

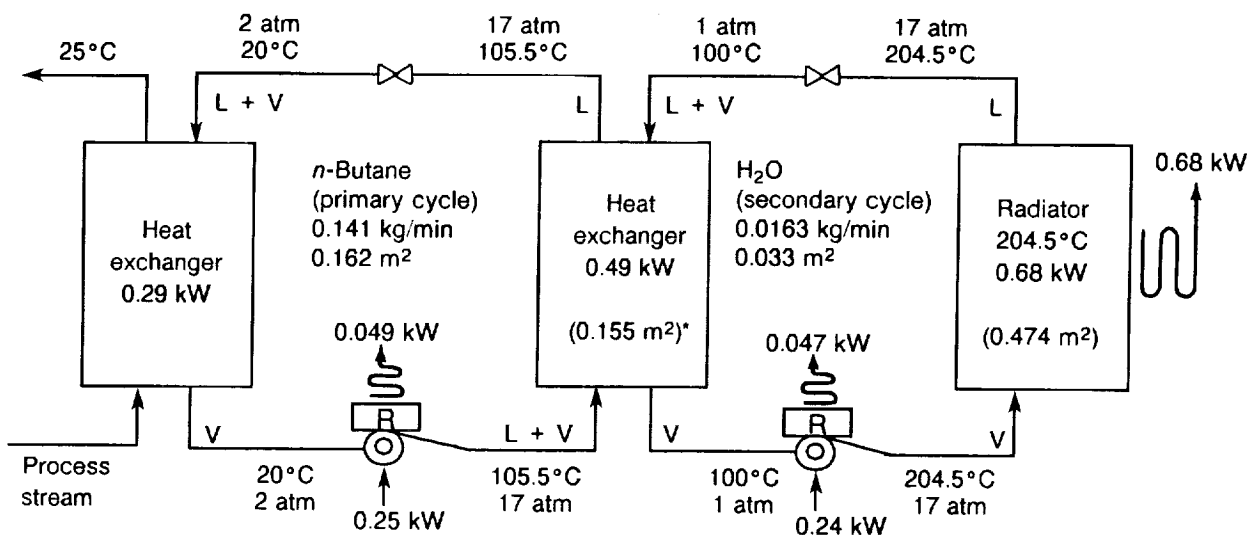
Refrigeration and Heat Radiation

The flowsheet for the refrigeration system used for method 1 cooling is shown in figure 18. The numerical values given are for a heat rejection rate of 0.29 kW. These values may be multiplied by the factor $Q/0.29$ to obtain correct values for any desired heat rejection rate of Q (kW).

Figure 18

Refrigerative Cooling Method (Dual Cycle)

-  = compressor + radiator (compressor efficiency taken as 80%)
-  = expander
- L = liquid phase present
- V = vapor phase present



* For heat transfer between fluids

The liquid *n*-butane absorbs the heat at 20°C (2 atm), vaporizes, and is compressed to 17 atm (105.5°C). The stream gives up its latent heat to liquid water at 100°C (1 atm) and condenses at 105.5°C (17 atm). Upon flowing through the expander, the *n*-butane partially evaporates until its temperature and pressure are lowered to 20°C (2 atm). It is then returned to the heat exchanger where the cycle is repeated.

The water cycle operates similarly but condenses within the radiator at 204.5°C (17 atm) before it is recycled. The radiator operates continuously at this temperature. We assumed that the radiators would be stationary and lie parallel to the lunar surface, exposed to the full radiation of the overhead Sun (lunar midday)—an extremely conservative assumption.

The radiator material is assumed to have an absorptivity of 0.35 and an emissivity of 0.77. The heat rejection rates for this type of radiator are taken from "Lunar Logistic System" (MSFC 1963). The reported values are based on an estimated 80-percent efficiency. The radiator mass factors used in our estimates were 6.1 kg/m² surface area for a plain radiator, and 19.5 kg/m² surface area for a

radiator with refrigeration. This latter value was also used for systems in which fluids condense or cool in tubes within or attached to the radiator. The 19.5 mass factor was obtained from "Lunar Logistic System" (MSFC 1963).

Compressor efficiencies are taken as 80 percent. The extra power required is rejected as heat from radiators attached to the compressors. Weights of standard compressor and motor units selected for use here were reduced by assuming that nonelectrical parts could be fabricated from lightweight aluminum alloys.

Refrigeration is not needed in method 2. The assumption is made that the radiator sees ~ 0 K space, either by being perpetually shadowed (for example, when located in depressions near the poles) or by being movable so as to present only an edge to the direct rays of the Sun. An iron-clad aluminum radiator would provide an emissivity of about 0.5 in a lightweight body. Reflectors on its underside and edge would prevent pickup of most of the radiation from the Moon's surface and from the Sun. The mass factor is taken as 9.8 kg/m² of surface. Once again, an 80-percent efficiency factor was used.

Total System Weight and Power

Table 6 lists the total system weights and power requirements for lunar oxygen plants of three capacities, using method 1 (refrigerative cooling). Table 7 does the same for method 2 (radiative cooling). The differences

in weight and power requirements for the two methods are striking, indicating that heat rejection techniques are of major importance in lunar plant design. (See Abe Hertzberg's paper in volume 2, "Thermal Management in Space.") In either case, scaling factors remain about constant.

TABLE 6. *Lunar Oxygen Plant Mass and Power Requirements, Using Refrigerative Cooling (Method 1)*

Section	Plant capacity (kg of O ₂ /Earth month)		
	2 720	5 440	10 880
Silicate reduction reactor, kg	344	533	943
Carbon monoxide reduction reactor, kg	415	829	1 659
Water electrolysis unit, kg	853	1 688	3 358
Oxygen liquefaction, kg	1 432	2 504	3 577
Refrigeration compressors, kg	<u>445</u>	<u>789</u>	<u>1 406</u>
Subtotal mass, kg	3 489	6 343	10 943
Liquid oxygen storage, kg	<u>1 173</u>	<u>2 345</u>	<u>4 690</u>
Total mass, kg	4 662	8 688	15 633
Silicate reduction reactor, kW	57.5	107.3	204.4
Water electrolysis unit, kW	28.0	56.0	112.0
Oxygen liquefaction, kW	7.5	15.0	22.5
Refrigeration compressors, kW	<u>38.4</u>	<u>76.8</u>	<u>140.9</u>
Total power, kW	131.4	255.1	479.8

TABLE 7. Lunar Oxygen Plant Mass and Power Requirements, Using Radiative Cooling (Method 2)

Section	Plant capacity (kg of O ₂ /Earth month)		
	2 720	5 440	10 880
Silicate reduction reactor, kg	344	533	943
Carbon monoxide reduction reactor, kg	278	555	1 110
Water electrolysis unit, kg	435	854	1 691
Oxygen liquefaction, kg	<u>1 327</u>	<u>2 293</u>	<u>3 261</u>
Subtotal mass, kg	2 384	4 235	7 005
Liquid oxygen storage, kg	<u>1 173</u>	<u>2 345</u>	<u>4 690</u>
Total mass, kg	3 557	6 580	11 695
Silicate reduction reactor, kW	57.5	107.3	204.4
Water electrolysis unit, kW	28.0	56.0	112.0
Oxygen liquefaction, kW	<u>7.5</u>	<u>15.0</u>	<u>22.5</u>
Total power, kW	93.0	178.3	338.9

This study indicates that a lunar plant employing the Aerojet carbothermal process to produce 2720 kg of oxygen per month would have a mass of approximately 4660 kg and require 132 kW_e using refrigeration cooling; a similar plant using radiative cooling exclusively would have a mass of approximately 3561 kg and require 93 kW_e. All estimates are based on a conservative approach to the problem.

Labor Estimates

We estimate that it will take no more than 8 hours' work to operate and maintain any of the three plants under study for 24 hours. One month of plant operation will require 240 work-hours. Based on a cost of \$500 000/work-hour, the labor cost for the manufacture of 1 kg of oxygen using the 2 720-kg, 5 440-kg, and 10 880-kg capacity plants is \$44 000, \$22 000, and \$11 000, respectively (1989 dollars).

Cost Comparisons

The dollar costs for the manufacture of oxygen on the Moon can be compared with the cost of delivering oxygen from the Earth by using a labor cost of \$500 000/work-hour and a transport cost of \$54 000/kg of

payload. This cost comparison is given in table 8. The manufacture of 2720 kg of oxygen per month for 1 year would cost \$1.71 billion (method 1, most conservative estimate), while the transport of an equivalent amount of oxygen would cost \$1.80 billion.

TABLE 8. *Cost* Comparison: Lunar Oxygen Manufacture Versus Earth-Moon Oxygen Transport (1-Year Cost Savings)*

Plant capacity, kg O ₂ /Earth month	2 720	5 440	10 880
Kilograms of O ₂ per year	32 640	65 280	130 560
\$Cost of delivered O ₂ ^a	1 770 x 10 ⁶	3 536 x 10 ⁶	7 079 x 10 ⁶
\$Cost of plant delivery ^{a,c}	251 x 10 ⁶	472 x 10 ⁶	846 x 10 ⁶
\$Cost of labor ^b	1 430 x 10 ⁶	1 430 x 10 ⁶	1 430 x 10 ⁶
\$Saved by lunar O ₂ plant ^c	88 x 10 ⁶	1 637 x 10 ⁶	4 803 x 10 ⁶
\$Saved by lighter lunar O ₂ plant ^d	147 x 10 ⁶	1 750 x 10 ⁶	5 088 x 10 ⁶

*Original 1965 dollars have been converted to 1989 dollars using the NASA R&D inflation factor of 4.916 (~5).

^aDelivery cost of \$54 000/kg

^bLabor cost of \$500 000/work-hour for 1/3 year

^cRefrigerative cooling, method 1

^dRadiative cooling, method 2

The cost of storing oxygen on the Moon is included in the cost of manufactured oxygen but not in the cost of transported oxygen. Utilizing propellant tanks from lunar landing vehicles to store oxygen on the Moon would reduce the cost of manufactured oxygen but not affect the cost of transported oxygen. If the storage cost were not included, the cost difference would be greater.

The data reported in table 8 dramatically indicate that much greater dollar savings will be realized by the manufacture of propellant oxygen on the Moon as the oxygen requirements are increased above 2720 kg/month.

Conclusion

We have shown with laboratory experimentation that the Aerojet carbothermal process is feasible. Natural silicates can be reduced with carbon or methane (see Rosenberg et al. 1965c for methane results). The important products are carbon monoxide, metal, and slag. The carbon monoxide can be completely reduced to form methane and water. The water can be electrolyzed to produce hydrogen and oxygen. A preliminary engineering study shows that the operation of plants using this process for the manufacture of propellant oxygen has a large

economic advantage when the cost of the plant and its operation is compared to the cost of delivering oxygen from Earth.

Bibliography

Marshall Space Flight Center. 1963. Lunar Logistic System, Vol. X, Payloads. Report MTP-M-63-1, March.

Rosenberg, S. D.; G. A. Guter; F. E. Miller; and G. R. Jameson. 1963. Research on Processes for Utilization of Lunar Resources. Aerojet-General Summary Report 2757, Contract NAS 7-225, Dec.; see also Catalytic Reduction of Carbon Monoxide with Hydrogen, NASA CR [Contractor Report] 57, July 1964.

Rosenberg, S. D.; G. A. Guter; and F. E. Miller. 1964a. Research on Processes for Utilization of Lunar Resources. Aerojet-General Summary Report 2895, Contract NAS 7-225, Aug.

Rosenberg, Sanders D.; Gerald A. Guter; and Michael Rothenberg. 1964b. Requirements for On-Site Manufacture of Propellant Oxygen from Lunar Raw Materials. Presented at 3rd Annual Meeting of the Working Group on Extraterrestrial Resources, Cocoa Beach, FL, Nov. 19.

Rosenberg, Sanders D.; Gerald A. Guter; and Frederick E. Miller. 1965a. Manufacture of Oxygen from Lunar Materials. *Ann. N.Y. Acad. Sci.* **123**:1106-1122.

Rosenberg, S. D.; G. A. Guter; F. E. Miller, and R. L. Beegle, Jr. 1965b. Research on Processes for Utilization of Lunar Resources. Aerojet-General Summary Report 3096, Contract NAS 7-225, Aug.

Rosenberg, S. D.; R. L. Beegle, Jr.; G. A. Guter; F. E. Miller; and M. Rothenberg. 1965c. The Manufacture of Propellants for the Support of Advanced Lunar Bases. Paper 650835 presented at the Society of Automotive Engineers' National Aeronautic and Space Engineering and Manufacturing Meeting, Los Angeles, Oct. 4-8.

Rosenberg, Sanders D. 1985. A Lunar-Based Propulsion System. In *Lunar Bases and Space Activities of the 21st Century*, ed. W. W. Mendell, 169-176. Houston: Lunar & Planetary Inst.

Rosenberg, S. D., and J. M. Halligan. 1988. The HELIOX Factory: Concepts for Lunar Resource Utilization. Paper LBS-88-124 presented at 2nd Symp. Lunar Bases & Space Activities of the 21st Century, sponsored by NASA, Lunar & Planetary Inst., AIAA, & others, Houston, Apr. 5-7.